



Imaging Pulmonary Infection: Classic Signs and Patterns

Christopher M. Walker¹
 Gerald F. Abbott¹
 Reginald E. Greene¹
 Jo-Anne O. Shepard¹
 Dharshan Vummidi²
 Subba R. Digumarthy¹

OBJECTIVE. The purposes of this article are to describe common and uncommon imaging signs and patterns of pulmonary infections and to discuss their underlying anatomic and pathophysiologic basis.

CONCLUSION. Imaging plays an integral role in the diagnosis and management of suspected pulmonary infections and may reveal useful signs on chest radiographs and CT scans. Detected early, these signs can often be used to predict the causative agent and pathophysiologic mechanism and possibly to optimize patient care.

Pulmonary infections are among the most common infections encountered in outpatient and inpatient clinical care. According to the Centers for Disease Control and Prevention, influenza and pneumonia were combined as the eighth leading cause of death in the United States in 2011 [1]. Imaging studies are critical for the diagnosis and management of pulmonary infections. When the imaging manifestations of a known disease entity form a consistent pattern or characteristic appearance, those manifestations may be regarded as an imaging sign of that disease. Imaging signs by themselves are sometimes nonspecific and may also be manifestations of noninfectious diseases. Various imaging signs of thoracic infection can be clinically useful, sometimes suggesting a specific diagnosis and often narrowing the differential diagnosis. Clinical data, such as WBC count, results of microbiologic tests, and immune status, should be correlated with the imaging sign and any additional findings to facilitate an accurate diagnosis. The objectives of this article are to discuss common and uncommon signs and findings of pulmonary infection at radiography and CT, discuss the mechanisms and pathophysiologic factors that produce those findings, and highlight several noninfectious diseases that may present with similar findings. This review is divided into signs that are most commonly seen or associated with bacterial, viral, fungal, and parasitic infections.

Consolidation and Air Bronchogram Sign

Consolidation is an alveolar-filling process that replaces air within the affected airspaces, increasing in pulmonary attenuation and obscuring the margins of adjacent airways and vessels on radiographs and CT scans [2]. Consolidation is one of the more common manifestations of pulmonary infection, and its appearance is variable, dependent on the causative organism.

Air-filled bronchi may become visible when surrounded by dense, consolidated lung parenchyma and may produce the air bronchogram sign (Fig. 1), initially described by Felix Fleischner in 1948 [3, 4]. In normal lung, air-filled bronchi are not apparent on chest radiographs because they are surrounded by aerated lung parenchyma. In a patient with fever and cough, this sign suggests the diagnosis of pneumonia. Though the sign is most commonly seen with bacterial infection, any infection can manifest the air bronchogram sign. Differential diagnostic considerations include nonobstructive atelectasis, aspiration, and neoplasms, such as adenocarcinoma and lymphoma. One can differentiate atelectasis from pneumonia by looking for direct and indirect signs of volume loss, including bronchovascular crowding, fissural displacement, mediastinal shift, and diaphragmatic elevation. Detection of the air bronchogram sign argues against the presence of a central obstructing lesion.

Keywords: abscess, fungus, infection, signs

DOI:10.2214/AJR.13.11463

Received June 26, 2013; accepted after revision August 16, 2013.

¹Department of Radiology, Thoracic Imaging Division, Massachusetts General Hospital, 55 Fruit St, Boston, MA 02114. Address correspondence to C. M. Walker (walk0060@gmail.com).

²Department of Radiology, University of Michigan, Ann Arbor, MI.

This article is available for credit.

AJR 2014; 202:479–492

0361–803X/14/2023–479

© American Roentgen Ray Society

Silhouette Sign

The silhouette sign was initially described by Felson as a radiographic sign that enabled the anatomic localization of abnormalities on orthogonal chest radiographs [5]. The silhouette sign describes loss of a normal lung–soft-tissue interface (loss of silhouette) caused by any pathologic mechanism that replaces or displaces air within the lung parenchyma. The silhouette sign is produced on chest radiographs when the loss of interface occurs between structures in the same anatomic plane within an image. This sign is commonly applied to the interface between the lungs and the heart, mediastinum, chest wall, and diaphragm. Consolidation that extends to the border of an adjacent soft-tissue structure will obliterate its interface with that structure [5]. For example, lingular pneumonia obscures the left-heart border, and middle lobe pneumonia obscures the right-heart border, because the areas of consolidation and the respective heart borders are in the same anatomic plane (Fig. 2). Conversely, with lower lobe pneumonia, the heart border is preserved, but the ipsilateral hemidiaphragm is frequently obscured (silhouetted). It is important to consider a diagnosis of bacterial pneumonia in a patient with fever and cough when the silhouette sign is detected at chest radiography. Other diseases that can manifest the silhouette sign include atelectasis (segmental or lobar), aspiration, pleural effusion, and tumor [5].

Tree-in-Bud Sign

The small airways or terminal bronchioles are invisible on CT images because of their small size (< 2 mm) and thin walls (< 0.1 mm). They may become indirectly visible on CT images when filled with mucus, pus, fluid, or cells, forming impactions that resemble a budding tree with branching nodular V- and Y-shaped opacities that are referred to as the tree-in-bud sign [6–9] (Fig. 3). Because tree-in-bud opacities form in the center of the secondary pulmonary lobule, they characteristically spare the subpleural lung parenchyma, including that adjacent to interlobar fissures.

Although initially thought to be diagnostic of mycobacterial infection, the tree-in-bud sign may be an imaging manifestation of various infections caused by bacteria, fungi, parasites, and viruses [6, 8, 10]. Tree-in-bud opacities usually indicate infectious bronchiolitis or aspiration but are less commonly seen in other conditions, such as follicular bronchiolitis, chronic airways inflammation

(e.g., cystic fibrosis or immune deficiency), diffuse panbronchiolitis, and adenocarcinoma [11]. Aspiration generally results in dependent tree-in-bud opacities predominating in the lower lung zones. Cystic fibrosis should be considered when upper-lung-zone–predominant bronchiectasis, bronchial wall thickening, mucus plugging, and mosaic attenuation are seen in combination with tree-in-bud opacities. Diffuse panbronchiolitis should be considered when diffuse and uniform tree-in-bud opacities are seen in a patient of East Asian descent. Less commonly, the tree-in-bud sign may be a manifestation of vascular lesions (so-called vascular tree-in-bud), including embolized tumor or foreign material, due to the anatomic location of small arterioles as paired homologous structures that course alongside the small airways in the centrilobular aspect of the secondary pulmonary lobules [8, 12–15] (Fig. 4).

Bulging Fissure Sign

The bulging fissure sign represents expansive lobar consolidation causing fissural bulging or displacement by copious amounts of inflammatory exudate within the affected parenchyma. Classically associated with right upper lobe consolidation due to *Klebsiella pneumoniae* (Fig. 5), any form of pneumonia can manifest the bulging fissure sign. The sign is frequently seen in patients with pneumococcal pneumonia [16, 17]. The prevalence of this sign is decreasing, likely because of prompt administration of antibiotic therapy to patients with suspected pneumonia [18]. The bulging fissure sign is also less commonly detected in patients with hospital-acquired *Klebsiella* pneumonia than in those with community-acquired *Klebsiella* infection [19]. Other diseases that manifest a bulging fissure include any space-occupying process in the lung, such as pulmonary hemorrhage, lung abscess, and tumor.

Feeding Vessel Sign

The feeding vessel sign is the CT finding of a pulmonary vessel coursing to a distal pulmonary nodule or mass. This sign was originally thought to indicate hematogenous dissemination of disease [20, 21], but when it was studied on multiplanar reformatted images, most of the so-called feeding vessels were actually pulmonary veins coursing from the nodule, and the pulmonary arteries usually coursed around the nodule [22]. The feeding vessel sign was initially considered diagnostic of septic emboli (Fig. 6) but has

come to be recognized as a potential manifestation of other conditions, including metastasis, arteriovenous fistula, and pulmonary vasculitis [23]. Septic emboli should be considered when the feeding vessel sign is seen with cavitating and noncavitating nodules and subpleural wedge-shaped consolidation. The nodules usually have basal and peripheral predominance and vary in size [24]. Arteriovenous fistula is differentiated from septic emboli by the finding not only of a feeding artery but also of an enlarged draining vein.

Inhomogeneous Enhancement Sign and Cavitation

In a patient with pneumonia, the CT detection of inhomogeneous enhancement and cavitation suggests the presence of necrotizing infection [25, 26]. Pulmonary necrosis may become evident as hypoenhancing geographic areas of low lung attenuation that may be difficult to differentiate from adjacent pleural fluid [25] (Fig. 7). This finding is often seen before frank abscess formation and is a predictor of a prolonged hospital course [26]. A cavity is defined as abnormal lucency within an area of consolidation with or without an associated air-fluid level. Cavitation may be the result of suppurative or caseous necrosis or lung infarction. Importantly, cavitation does not always indicate a lung infection or abscess. Cavitation can have noninfectious causes, including malignancy, radiation therapy, and lung infarction [2]. Suppurative necrosis usually occurs with infection by *Staphylococcus aureus*, gram-negative bacteria, or anaerobes. Caseous necrosis is a characteristic histologic feature of mycobacterial infection, but cavitation is a common pathologic and imaging feature of angioinvasive fungal infections, such as aspergillosis and mucormycosis.

Air-Fluid Level Sign

In a patient with pneumonia, detection of an air-fluid level on chest radiographs or CT images suggests the presence of a lung abscess or empyema with bronchopleural fistula. The former typically requires medical treatment with antibiotics, and the latter usually requires insertion of a chest tube for drainage. Lung abscess is most commonly associated with aspiration pneumonia and septic pulmonary emboli. Common causative organisms include anaerobes, *Staphylococcus aureus*, and *Klebsiella pneumoniae*. Lung abscess is associated with increased morbidity and mortality. Prompt detection at imaging

Imaging Pulmonary Infection

studies may improve patient care, enabling clinicians to treat patients with an appropriate course of antibiotic therapy [27].

Detection of an air-fluid level at chest radiography should prompt evaluation of its location as being in the lung parenchyma or within the pleural space. A lung abscess with an air-fluid level can be differentiated from empyema with bronchopleural fistula by measurement and comparison of the lengths of the visualized air-fluid level on orthogonal chest radiographs. Because of the characteristic spherical shape of a lung abscess, an associated air-fluid level typically has equal lengths on posteroanterior and lateral chest radiographs (Fig. 8). By contrast, empyema typically forms lenticular collections of pleural fluid, and an associated air-fluid level (e.g., bronchopleural fistula) usually exhibits length disparity when compared on posteroanterior and lateral chest radiographs. In addition, both entities typically display a difference in the angle of their interface with an adjacent pleural surface. A lung abscess usually forms an acute angle when it intersects with an adjacent pleural surface, and its wall is often thick and irregular. By contrast, empyema typically forms obtuse angles along its interface with adjacent pleura and usually has smooth, thin, enhancing walls [28, 29]. Other differential diagnostic considerations for an intrathoracic air-fluid level include hemorrhage into a cavity, lung cancer, and metastatic disease.

Split-Pleura Sign

Normal visceral and parietal pleura are indistinguishable on CT images. In the presence of an exudative pleural effusion with loculation, inflammatory changes may thicken both the visceral and parietal pleura that surround the fluid collection and may become evident as the split-pleura sign, suggesting the presence of empyema [28, 30]. A loculated effusion may have an atypical chest radiographic appearance when located within a fissure. The split-pleura sign may be seen in combination with the air-fluid level sign when a bronchopleural fistula occurs within empyema.

Empyema should be considered when a patient presents with fever, cough, and chest pain and CT shows the split-pleura sign. In a series of 58 patients with empyema, the split-pleura sign was seen in 68% [30] (Fig. 9). The split-pleura sign is not specific for empyema but rather indicates the presence of an exudative effusion [31]. Other important causes of this sign include parapneumonic and malig-

nant effusions (Fig. 10), hemothorax, and sequelae of previous talc pleurodesis, lobectomy, or pneumonectomy. Hemothorax usually has associated heterogeneously high attenuation, and talc pleurodesis has attenuation similar to that of calcium and is often clumped.

Halo Sign

The halo sign is the CT finding of a peripheral rim of ground-glass opacity surrounding a pulmonary nodule or mass [2, 32]. When detected in a febrile patient with neutropenia, this sign is highly suggestive of angioinvasive *Aspergillus* infection [32–34] (Fig. 11). The ground-glass opacity represents hemorrhage surrounding infarcted lung and is caused by vascular invasion by the fungus [35]. The halo sign is typically seen early in the course of the infection. In a group of 25 patients with invasive *Aspergillus* infection, the halo sign was seen in 24 patients on day 0 and was detected in only 19% of patients by day 14, highlighting the importance of performing CT early in the course of a suspected fungal infection [36]. In a large group of immunocompromised patients with *Aspergillus* infection, Greene and colleagues [37] found that patients in whom the halo sign was visualized at CT had improved survival and response to antifungal treatment compared with those without the halo sign at CT. Differential considerations for the halo sign include other infections, such as mucormycosis and *Candida* (Fig. 12), *Pseudomonas*, herpes simplex virus, and cytomegalovirus infections, and other causes, such as Wegener granulomatosis, hemorrhagic metastasis, and Kaposi sarcoma [38, 39].

Air Crescent Sign of Angioinvasive *Aspergillus* Infection

The air crescent sign is the CT finding of a crescentic collection of air that separates a nodule or mass from the wall of a surrounding cavity [2]. This sign is seen in two types of *Aspergillus* infection: angioinvasive and mycetoma [40]. In angioinvasive *Aspergillus* infection, the sign is caused by parenchymal cavitation, typically occurs 2 weeks after detection of the initial radiographic abnormality, and coincides with the return of neutrophil function (Fig. 13). The air crescent sign is suggestive of a favorable patient prognosis [41]. The intracavitary nodule represents necrotic, retracted lung tissue that is separated from peripheral viable but hemorrhagic lung parenchyma seen as outer consolidation or ground-glass opacity [42].

Air Crescent or Monad Sign of Mycetoma

The air crescent sign of mycetoma, also referred to as the Monad sign, is seen in an immunocompetent host with preexisting cystic or cavitary lung disease, usually from tuberculosis or sarcoidosis [42]. The fungal ball or mycetoma develops within a preexisting lung cavity and may exhibit gravity dependence (Fig. 14). The mycetoma is composed of fungal hyphae, mucus, and cellular debris. Mycetomas can cause hemoptysis. The treatment options include surgical resection, bronchial artery embolization, and instillation of antifungal agents into the cavity [40]. The air crescent sign is not specific for *Aspergillus* infection and can be seen in other conditions, such as cavitating neoplasm, intracavitary clot, and Wegener granulomatosis [2, 43, 44].

Finger-in-Glove Sign

The finger-in-glove sign is the chest radiographic finding of tubular and branching tubular opacities that appear to emanate from the hila, said to resemble gloved fingers [45, 46]. The tubular opacities represent dilated bronchi impacted with mucus. The CT finger-in-glove sign is branching endobronchial opacities that course alongside neighboring pulmonary arteries. The finding is classically associated with allergic bronchopulmonary aspergillosis (ABPA), seen in persons with asthma and patients with cystic fibrosis (Fig. 15), but may also occur as an imaging manifestation of endobronchial tumor (Fig. 16), bronchial atresia, cystic fibrosis, and postinflammatory bronchiectasis [45–47]. Bronchoscopy may be necessary to exclude endobronchial tumor as the cause of the finger-in-glove sign.

The tubular opacities that occur in ABPA result from hyphal masses and mucoid impaction and typically affect the upper lobes. In 19–28% of cases, the endobronchial opacities in ABPA may be calcified or hyperattenuating on unenhanced CT images (Fig. 15), probably because of the presence of calcium salts, metals, and desiccated mucus [47–50].

Crazy-Paving Sign

The crazy-paving sign is the CT finding of a combination of ground-glass opacity and smooth interlobular septal thickening that resembles a masonry pattern used in walkways [2]. The crazy-paving sign was originally described as a characteristic CT pattern detected in patients with pulmonary alveolar proteinosis. The sign has come to be recognized, however, as occurring in many other condi-

tions, including infection (e.g., *Pneumocystis jiroveci* pneumonia, influenza, and infections by other organisms) [51, 52]. In *Pneumocystis* pneumonia, the histologic features that produce the crazy-paving pattern are alveolar exudates containing the infective organisms and cellular infiltration or edema in the alveolar walls and interlobular septa [52, 53]. Ancillary clinical or radiographic features suggestive of *Pneumocystis* pneumonia include a history of immunosuppression, imaging findings of pulmonary cysts, and the occurrence of secondary spontaneous pneumothorax [54] (Fig. 17).

Differential diagnostic considerations for the crazy-paving sign can be categorized according to the typical time course of the suspected diseases (Fig. 18). Diseases characterized by an acute time course include pulmonary edema, pulmonary hemorrhage, and infection. Those with a more chronic course include pulmonary alveolar proteinosis, pulmonary adenocarcinoma, and lipoid pneumonia [52, 55].

Grape-Skin Sign

The grape-skin sign is the radiographic or CT finding of a very thin-walled cavitory lesion that develops in lung parenchyma previously affected by consolidation or lung granulomas that have undergone central caseous necrosis [56]. As classically described, the grape-skin sign is a solitary finding of a thin-walled cavity with central lucency that has been associated with chronic pulmonary coccidioidomycosis infection [57, 58] (Fig. 19). Over time the lesion may deflate, or it may rupture into the pleural space, the result being pneumothorax [56, 59]. The differential diagnosis of this finding includes other solitary cavitory or cystic lesions, such as reactivation tuberculosis infection, pneumatocele, neoplasm (e.g., primary lung cancer or metastasis), and other fungal infections.

Miliary Pattern

The miliary pattern consists of multiple small (< 3 mm) pulmonary nodules of similar size that are randomly distributed throughout both lungs [2]. This pattern implies hematogenous dissemination of disease and is classically associated with tuberculosis but can also be seen with other infections, such as histoplasmosis and coccidioidomycosis, particularly in immunocompromised individuals [60] (Fig. 20). Random pulmonary nodules must be differentiated from those with a centrilobular or perilymphatic distribution. Cen-

trilobular nodules are evenly spaced and do not come into contact with adjacent pleural surfaces. Perilymphatic nodules are distributed along peribronchovascular structures, the subpleural lung, and along interlobular septa. Random nodules forming the miliary pattern are distributed uniformly throughout the lungs, and those in the periphery may come into contact with a pleural surface [61, 62]. Noninfectious causes of the miliary pattern include metastatic disease, IV injected foreign material, and rarely sarcoidosis [62, 63].

Reverse Halo and Bird's Nest Signs

The reverse halo sign is the CT finding of peripheral consolidation surrounding a central area of ground-glass opacity [64]. Associated irregular and intersecting areas of stranding or irregular lines may be present within the area of ground-glass opacity and become evident as the bird's nest sign [65] (Fig. 21). These signs are suggestive of invasive fungal infection (e.g., angioinvasive *Aspergillus* infection or mucormycosis) in susceptible patient populations [66]. Major predisposing factors for fungal infection include stem cell or solid organ transplant, hematologic malignancy, diabetic ketoacidosis, and a depressed immune system. Imaging features that favor mucormycosis over *Aspergillus* infection in a neutropenic patient are detection of the reverse halo or bird's nest sign, multiplicity of pulmonary nodules (> 10), and development of infection despite voriconazole prophylaxis [66–68]. The reverse halo and bird's nest signs are not specific for invasive fungal infection and may also be seen in other conditions, including cryptogenic organizing pneumonia, bacterial pneumonia, paracoccidioidomycosis, tuberculosis, sarcoidosis, Wegener granulomatosis, and pulmonary infarction [64, 68–73].

Meniscus, Cumbo, and Water Lily Signs of Echinococcal Infection

Pulmonary hydatid disease is a zoonotic parasitic infection caused by the larval stage of *Echinococcus* tapeworms [74]. This genus of worms is endemic in Alaska, South America, the Mediterranean region, Africa, and Australia. Humans can serve as intermediate hosts after contact with a definitive host (e.g., dog or wolf) or after consuming contaminated vegetables or water [74]. The lung is the second most common organ involved, after the liver, and is infected by either hematogenous or direct transdiaphragmatic spread from the liver [74–76].

The hydatid cyst is composed of three layers: an outer protective barrier consisting of modified host cells, called the pericyst; a middle acellular laminated membrane, called the ectocyst; and an inner germinal layer that produces scolices, hydatid fluid, daughter vesicles, and daughter cysts, called the endocyst [74, 75, 77]. The meniscus, Cumbo, and water lily signs are all seen with pulmonary echinococcal infection [74–78]. These signs are caused by air dissecting between the cyst layers, which are initially indistinguishable on CT images because the cysts are fluid filled (Fig. 22). With bronchial erosion, air dissects between the outer pericyst and ectocyst to produce the meniscus sign (Fig. 23). Some radiologists believe that the meniscus sign is suggestive of impending cyst rupture [76, 77]. As it accumulates further, air penetrates the endocyst layer and causes the Cumbo sign, which comprises an air-fluid level in the endocyst and a meniscus sign (Fig. 23). Finally, the endocyst layer collapses and floats on fluid, forming the water lily sign (Fig. 24).

Burrow Sign of Paragonimiasis

Paragonimiasis is a zoonotic parasitic infection caused by lung flukes [79]. Humans serve as a definitive host when they ingest raw or improperly cooked crab or crayfish [76]. *Paragonimus westermani* and *Paragonimus kellicotti* are the two pathogens endemic to Asia and North America, respectively. They produce similar imaging findings in the thorax [79–83].

The chest CT findings reflect the life cycle of the parasite. The second form of the immature organism lives in the crab or crayfish. After ingestion by a mammal, the parasite penetrates through the small bowel to enter the peritoneal cavity, where it incites an inflammatory reaction. Several weeks later, the organism migrates through the diaphragm to enter the pleural space. After finding mates, the parasites burrow through the visceral pleura into the lung parenchyma, where they produce cysts that contain eggs. The eggs are extruded into bronchioles and expectorated by the infected mammal to complete the life cycle [79]. The burrow sign is a linear track extending from the pleural surface or hemidiaphragm to a cavitory or cystic pulmonary nodule. The linear track represents the path followed by the worms within the lung, and the cavitory or cystic pulmonary nodule contains both the adult worms and their eggs (Fig. 25). There is often associated pleural effusion, omental fat

Imaging Pulmonary Infection

stranding, and anterior cardiophrenic and internal mammary lymphadenopathy. Patients occasionally present with pneumothorax [79–83]. Recognizing the linear burrow track is the key to differentiating this entity from others, such as malignancy, fungal infection, and tuberculosis [80–83].

Conclusion

Imaging plays an important role in the diagnosis of suspected pulmonary infection and may reveal useful signs at chest radiography and CT. Signs such as the water lily and burrow signs almost always indicate a specific infection, whereas findings such as the split-pleura sign often suggest a specific diagnosis of empyema in the clinical setting of pneumonia. Several signs, such as the halo and reverse halo signs, may indicate potentially serious fungal infections in an immunocompromised patient. Imaging signs of lung abscess, such as the air-fluid level sign in a cavity, may also be predictive of prognosis and guide duration of therapy.

References

1. Hoyert DL, Xu J. Deaths: preliminary data for 2011. *Natl Vital Stat Rep* 2012; 61:1–51
2. Hansell DM, Bankier AA, MacMahon H, McLoud TC, Müller NL, Remy J. Fleischner Society: glossary of terms for thoracic imaging. *Radiology* 2008; 246:697–722
3. Fleischner FG. The visible bronchial tree; a roentgen sign in pneumonic and other pulmonary consolidations. *Radiology* 1948; 50:184–189
4. Fleischner FG. Der sichtbare Bronchialbaum, ein differentialdiagnostisches Symptom im Röntgenbild der Pneumonia. *Fortschr Geb Rontgenstr* 1927; 36:319–323
5. Felson B, Felson H. Localization of intrathoracic lesions by means of the postero-anterior roentgenogram; the silhouette sign. *Radiology* 1950; 55:363–374
6. Verma N, Chung JH, Mohammed TL. Tree-in-bud sign. *J Thorac Imaging* 2012; 27:W27
7. Eisenhuber E. The tree-in-bud sign. *Radiology* 2002; 222:771–772
8. Rossi SE, Franquet T, Volpacchio M, Giménez A, Aguilar G. Tree-in-bud pattern at thin-section CT of the lungs: radiologic-pathologic overview. *RadioGraphics* 2005; 25:789–801
9. Collins J, Blankenbaker D, Stern EJ. CT patterns of bronchiolar disease: what is “tree-in-bud”? *AJR* 1998; 171:365–370
10. Im JG, Itoh H, Shim YS, et al. Pulmonary tuberculosis: CT findings—early active disease and sequential change with antituberculous therapy. *Radiology* 1993; 186:653–660
11. Li Ng Y, Hwang D, Patsios D, Weisbrod G. Tree-in-bud pattern on thoracic CT due to pulmonary intravascular metastases from pancreatic adenocarcinoma. *J Thorac Imaging* 2009; 24:150–151
12. Franquet T, Giménez A, Prats R, Rodríguez-Arias JM, Rodríguez C. Thrombotic microangiopathy of pulmonary tumors: a vascular cause of tree-in-bud pattern on CT. *AJR* 2002; 179:897–899
13. Bendeck SE, Leung AN, Berry GJ, Daniel D, Ruoss SJ. Cellulose granulomatosis presenting as centrilobular nodules: CT and histologic findings. *AJR* 2001; 177:1151–1153
14. Tack D, Nollevaux MC, Gevenois PA. Tree-in-bud pattern in neoplastic pulmonary emboli. *AJR* 2001; 176:1421–1422
15. Shepard JA, Moore EH, Templeton PA, McLoud TC. Pulmonary intravascular tumor emboli: dilated and beaded peripheral pulmonary arteries at CT. *Radiology* 1993; 187:797–801
16. Francis JB, Francis PB. Bulging (sagging) fissure sign in *Hemophilus influenzae* lobar pneumonia. *South Med J* 1978; 71:1452–1453
17. Felson B, Rosenberg LS, Hamburger M. Roentgen findings in acute Friedländer’s pneumonia. *Radiology* 1949; 53:559–565
18. Korvick JA, Hackett AK, Yu VL, Muder RR. Klebsiella pneumonia in the modern era: clinico-radiographic correlations. *South Med J* 1991; 84:200–204
19. Rafat C, Fihman V, Ricard JD. A 51-year-old man presenting with shock and lower-lobe consolidation with interlobar bulging fissure. *Chest* 2013; 143:1167–1169
20. Kuhlman JE, Fishman EK, Teigen C. Pulmonary septic emboli: diagnosis with CT. *Radiology* 1990; 174:211–213
21. Huang RM, Naidich DP, Lubat E, Schinella R, Garay SM, McCauley DI. Septic pulmonary emboli: CT-radiographic correlation. *AJR* 1989; 153:41–45
22. Dodd JD, Souza CA, Müller NL. High-resolution MDCT of pulmonary septic embolism: evaluation of the feeding vessel sign. *AJR* 2006; 187:623–629
23. Milne EN, Zerhouni EA. Blood supply of pulmonary metastases. *J Thorac Imaging* 1987; 2:15–23
24. Han D, Lee KS, Franquet T, et al. Thrombotic and nonthrombotic pulmonary arterial embolism: spectrum of imaging findings. *RadioGraphics* 2003; 23:1521–1539
25. Ketai L, Jordan K, Marom EM. Imaging infection. *Clin Chest Med* 2008; 29:77–105
26. Donnelly LF, Klosterman LA. Pneumonia in children: decreased parenchymal contrast enhancement—CT sign of intense illness and impending cavitary necrosis. *Radiology* 1997; 205: 817–820
27. Hirshberg B, Sklair-Levi M, Nir-Paz R, Ben-Sira L, Krivoruk V, Kramer MR. Factors predicting mortality of patients with lung abscess. *Chest* 1999; 115:746–750
28. Kuhlman JE, Singha NK. Complex disease of the pleural space: radiographic and CT evaluation. *RadioGraphics* 1997; 17:63–79
29. Kuhlman JE. Complex disease of the pleural space: the 10 questions most frequently asked of the radiologist—new approaches to their answers with CT and MR imaging. *RadioGraphics* 1997; 17:1043–1050
30. Stark DD, Federle MP, Goodman PC, Podrasky AE, Webb WR. Differentiating lung abscess and empyema: radiography and computed tomography. *AJR* 1983; 141:163–167
31. Aquino SL, Webb WR, Gushiken BJ. Pleural exudates and transudates: diagnosis with contrast-enhanced CT. *Radiology* 1994; 192:803–808
32. Pinto PS. The CT halo sign. *Radiology* 2004; 230:109–110
33. Kuhlman JE, Fishman EK, Siegelman SS. Invasive pulmonary aspergillosis in acute leukemia: characteristic findings on CT, the CT halo sign, and the role of CT in early diagnosis. *Radiology* 1985; 157:611–614
34. Kuhlman JE, Fishman EK, Burch PA, Karp JE, Zerhouni EA, Siegelman SS. Invasive pulmonary aspergillosis in acute leukemia: the contribution of CT to early diagnosis and aggressive management. *Chest* 1987; 92:95–99
35. Won HJ, Lee KS, Cheon JE, et al. Invasive pulmonary aspergillosis: prediction at thin-section CT in patients with neutropenia—a prospective study. *Radiology* 1998; 208:777–782
36. Caillot D, Couaillier JF, Bernard A, et al. Increasing volume and changing characteristics of invasive pulmonary aspergillosis on sequential thoracic computed tomography scans in patients with neutropenia. *J Clin Oncol* 2001; 19:253–259
37. Greene RE, Schlamm HT, Oestmann JW, et al. Imaging findings in acute invasive pulmonary aspergillosis: clinical significance of the halo sign. *Clin Infect Dis* 2007; 44:373–379
38. Primack SL, Hartman TE, Lee KS, Müller NL. Pulmonary nodules and the CT halo sign. *Radiology* 1994; 190:513–515
39. Jamadar DA, Kazerooni EA, Daly BD, White CS, Gross BH. Pulmonary zygomycosis: CT appearance. *J Comput Assist Tomogr* 1995; 19:733–738
40. Buckingham SJ, Hansell DM. Aspergillus in the lung: diverse and coincident forms. *Eur Radiol* 2003; 13:1786–1800
41. Abramson S. The air crescent sign. *Radiology* 2001; 218:230–232
42. McAdams HP, Rosado-de-Christenson ML, Templeton PA, Lesar M, Moran CA. Thoracic mycoses from opportunistic fungi: radiologic-pathologic correlation. *RadioGraphics* 1995; 15:271–286

43. Bard R, Hassani N. Crescent sign in pulmonary hematoma. *Respiration* 1975; 32:247–251
44. Cubillo-Herguera E, McAlister WH. The pulmonary meniscus sign in a case of bronchogenic carcinoma. *Radiology* 1969; 92:1299–1300
45. Nguyen ET. The gloved finger sign. *Radiology* 2003; 227:453–454
46. Mintzer RA, Neiman HL, Reeder MM. Muroid impaction of a bronchus. *JAMA* 1978; 240:1397–1398
47. Agarwal R, Aggarwal AN, Gupta D. High-attenuation mucus in allergic bronchopulmonary aspergillosis: another cause of diffuse high-attenuation pulmonary abnormality. *AJR* 2006; 186:904
48. Agarwal R, Gupta D, Aggarwal AN, Saxena AK, Chakrabarti A, Jindal SK. Clinical significance of hyperattenuating muroid impaction in allergic bronchopulmonary aspergillosis: an analysis of 155 patients. *Chest* 2007; 132:1183–1190
49. Logan PM, Müller NL. High-attenuation mucous plugging in allergic bronchopulmonary aspergillosis. *Can Assoc Radiol J* 1996; 47:374–377
50. Agarwal R. High attenuation muroid impaction in allergic bronchopulmonary aspergillosis. *World J Radiol* 2010; 2:41–43
51. Murch CR, Carr DH. Computed tomography appearances of pulmonary alveolar proteinosis. *Clin Radiol* 1989; 40:240–243
52. Rossi SE, Erasmus JJ, Volpacchio M, Franquet T, Castiglioni T, McAdams HP. “Crazy-paving” pattern at thin-section CT of the lungs: radiologic-pathologic overview. *RadioGraphics* 2003; 23:1509–1519
53. Marchiori E, Müller NL, Soares Souza A, Escuisato DL, Gasparetto EL, Franquet T. Pulmonary disease in patients with AIDS: high-resolution CT and pathologic findings. *AJR* 2005; 184:757–764
54. Kanne JP, Yandow DR, Meyer CA. *Pneumocystis jirovecii* pneumonia: high-resolution CT findings in patients with and without HIV infection. *AJR* 2012; 198:[web]W555–W561
55. Franquet T, Giménez A, Bordes R, Rodríguez-Arias JM, Castella J. The crazy-paving pattern in exogenous lipid pneumonia: CT-pathologic correlation. *AJR* 1998; 170:315–317
56. McGahan JP, Graves DS, Palmer PE, Stadalnik RC, Dublin AB. Classic and contemporary imaging of coccidioidomycosis. *AJR* 1981; 136:393–404
57. Chong S, Lee KS, Yi CA, Chung MJ, Kim TS, Han J. Pulmonary fungal infection: imaging findings in immunocompetent and immunocompromised patients. *Eur J Radiol* 2006; 59:371–383
58. Kim KI, Leung AN, Flint JD, Müller NL. Chronic pulmonary coccidioidomycosis: computed tomographic and pathologic findings in 18 patients. *Can Assoc Radiol J* 1998; 49:401–407
59. McAdams HP, Rosado-de-Christenson ML, Lesar M, Templeton PA, Moran CA. Thoracic mycoses from endemic fungi: radiologic-pathologic correlation. *RadioGraphics* 1995; 15:255–270
60. Burrill J, Williams CJ, Bain G, Conder G, Hine AL, Misra RR. Tuberculosis: a radiologic review. *RadioGraphics* 2007; 27:1255–1273
61. Gruden JF, Webb WR, Naidich DP, McGuinness G. Multinodular disease: anatomic localization at thin-section CT—multireader evaluation of a simple algorithm. *Radiology* 1999; 210:711–720
62. Lee KS, Kim TS, Han J, et al. Diffuse micronodular lung disease: HRCT and pathologic findings. *J Comput Assist Tomogr* 1999; 23:99–106
63. Koyama T, Ueda H, Togashi K, Umeoka S, Kataoka M, Nagai S. Radiologic manifestations of sarcoidosis in various organs. *RadioGraphics* 2004; 24:87–104
64. Walker CM, Mohammed TL, Chung JH. Reversed halo sign. *J Thorac Imaging* 2011; 26:W80
65. Vogl TJ, Hinrichs T, Jacobi V, Böhme A, Hoelzer D. Computed tomographic appearance of pulmonary mucormycosis [in German]. *Rofo* 2000; 172:604–608
66. Georgiadou SP, Sipsas NV, Marom EM, Kontoyiannis DP. The diagnostic value of halo and reversed halo signs for invasive mold infections in compromised hosts. *Clin Infect Dis* 2011; 52:1144–1155
67. Chamilos G, Marom EM, Lewis RE, Lionakis MS, Kontoyiannis DP. Predictors of pulmonary zygomycosis versus invasive pulmonary aspergillosis in patients with cancer. *Clin Infect Dis* 2005; 41:60–66
68. Chung JH, Godwin JD, Chien JW, Pipavath SJ. Case 160: pulmonary mucormycosis. *Radiology* 2010; 256:667–670
69. Kim SJ, Lee KS, Ryu YH, et al. Reversed halo sign on high-resolution CT of cryptogenic organizing pneumonia: diagnostic implications. *AJR* 2003; 180:1251–1254
70. Gasparetto EL, Escuisato DL, Davaus T, et al. Reversed halo sign in pulmonary paracoccidioidomycosis. *AJR* 2005; 184:1932–1934
71. Marchiori E, Grando RD, Simões Dos Santos CE, et al. Pulmonary tuberculosis associated with the reversed halo sign on high-resolution CT. *Br J Radiol* 2010; 83:e58–e60
72. Marchiori E, Zanetti G, Mano CM, Hochhegger B, Irion KL. The reversed halo sign: another atypical manifestation of sarcoidosis. *Korean J Radiol* 2010; 11:251–252
73. Mango VL, Naidich DP, Godoy MC. Reversed halo sign after radiofrequency ablation of a lung nodule. *J Thorac Imaging* 2011; 26:W150–W152
74. Pedrosa I, Safz A, Arrazola J, Ferreira J, Pedrosa CS. Hydatid disease: radiologic and pathologic features and complications. *RadioGraphics* 2000; 20:795–817
75. Polat P, Kantarci M, Alper F, Suma S, Koruyucu MB, Okur A. Hydatid disease from head to toe. *RadioGraphics* 2003; 23:475–494
76. Martínez S, Restrepo CS, Carrillo JA, et al. Thoracic manifestations of tropical parasitic infections: a pictorial review. *RadioGraphics* 2005; 25:135–155
77. Balikian JP, Mudarris FF. Hydatid disease of the lungs: a roentgenologic study of 50 cases. *Am J Roentgenol Radium Ther Nucl Med* 1974; 122:692–707
78. McPhail JL, Arora TS. Intrathoracic hydatid disease. *Dis Chest* 1967; 52:772–781
79. Procop GW. North American paragonimiasis (caused by *Paragonimus kellicotti*) in the context of global paragonimiasis. *Clin Microbiol Rev* 2009; 22:415–446
80. Henry TS, Lane MA, Weil GJ, Bailey TC, Bhalla S. Chest CT features of North American paragonimiasis. *AJR* 2012; 198:1076–1083
81. Im JG, Whang HY, Kim WS, Han MC, Shim YS, Cho SY. Pleuropulmonary paragonimiasis: radiologic findings in 71 patients. *AJR* 1992; 159:39–43
82. Kim TS, Han J, Shim SS, et al. Pleuropulmonary paragonimiasis: CT findings in 31 patients. *AJR* 2005; 185:616–621
83. Im JG, Kong Y, Shin YM, et al. Pulmonary paragonimiasis: clinical and experimental studies. *RadioGraphics* 1993; 13:575–586

(Figures start on next page)

Imaging Pulmonary Infection

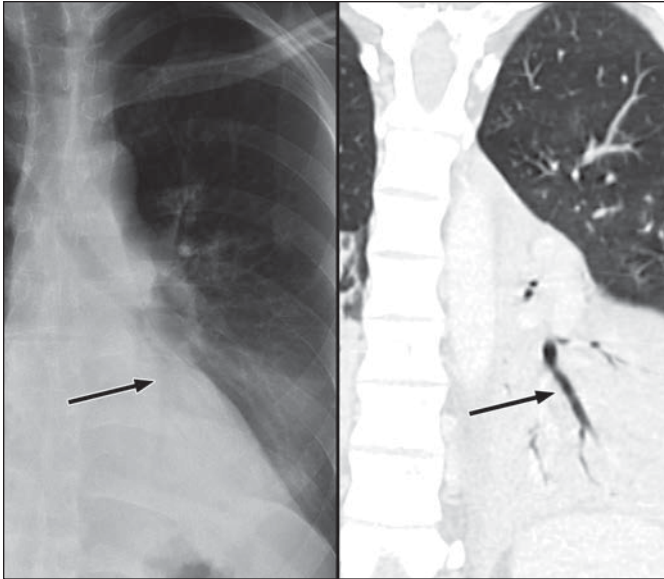


Fig. 1—49-year-old man with left lower lobe pneumonia. Example of air bronchogram sign. Posteroanterior radiograph (*left*) and coronal CT image (*right*) show left lower lobe consolidation and air bronchogram sign (*arrows*).

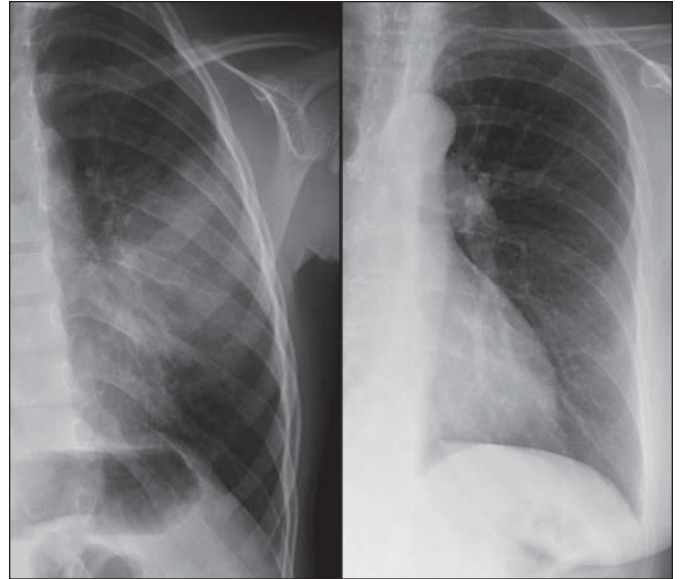


Fig. 2—4-year-old girl with lingular pneumonia. Example of silhouette sign. Posteroanterior radiographs show normal interface (*right*) and loss of normal interface of lung and left-heart border (*left*), thus localizing abnormality to lingula.

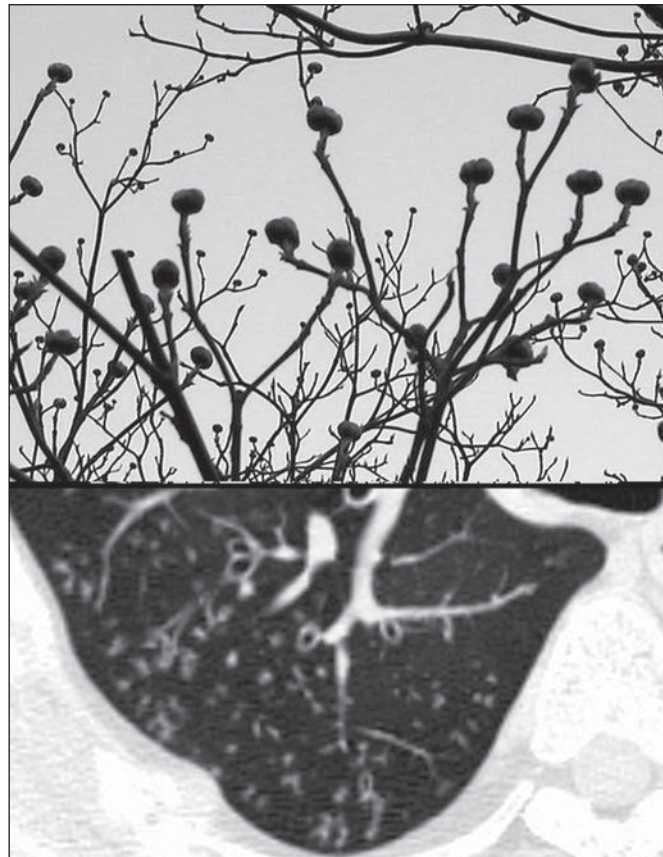


Fig. 3—45-year-old man with reactivation tuberculosis. Example of tree-in-bud sign. Photograph (*top*) shows budding tree. Axial CT image (*bottom*) shows numerous V- and Y-shaped tree-in-bud opacities.



Fig. 4—40-year-old man after IV injection of crushed morphine sulfate tablets. Example of tree-in-bud sign. Axial maximum-intensity-projection image shows diffuse vascular tree-in-bud opacities and dilated main pulmonary arteries. Similar findings involved all aspects of both lungs. Infectious bronchiolitis or aspiration is unlikely to result in such diffuse bilateral distribution of tree-in-bud opacities, and other conditions, such as diffuse panbronchiolitis and injection of foreign material, as in this case, should be considered as alternative diagnoses.

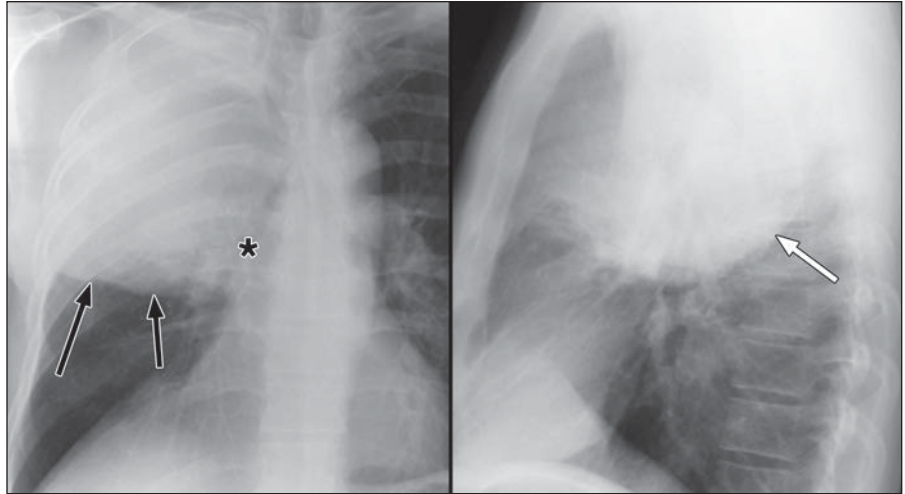


Fig. 5—75-year-old man with alcoholism and *Klebsiella* pneumonia. Example of bulging fissure sign. Posteroanterior (left) and lateral (right) radiographs show right upper lobe consolidation causing inferior bulging of minor fissure (black arrows), posterior bulging of major fissure (white arrow), and inferomedial displacement of bronchus intermedius (asterisk).

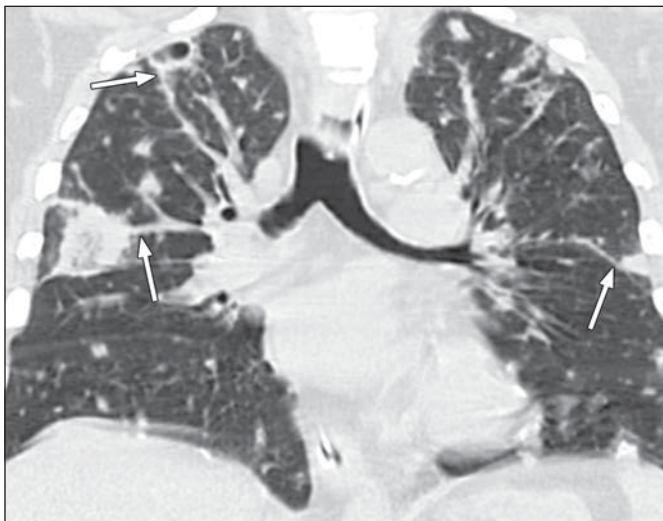


Fig. 6—45-year-old man with septic emboli. Example of feeding vessel sign. Coronal CT image shows septic pulmonary emboli manifesting themselves as peripheral solid and cavitary pulmonary nodules of varying sizes. Many nodules exhibit feeding vessel sign (arrows).

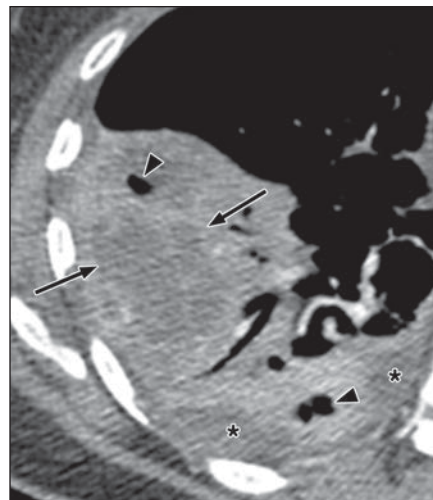


Fig. 7—55-year-old man with necrotizing aspiration pneumonia. Example of inhomogeneous enhancement. Axial contrast-enhanced CT image shows heterogeneously enhancing right lower lobe consolidation (arrows) suspicious for early pulmonary necrosis. Also present are foci of air (arrowheads) representing early abscess formation and small loculated right pleural effusion (asterisks).

Imaging Pulmonary Infection

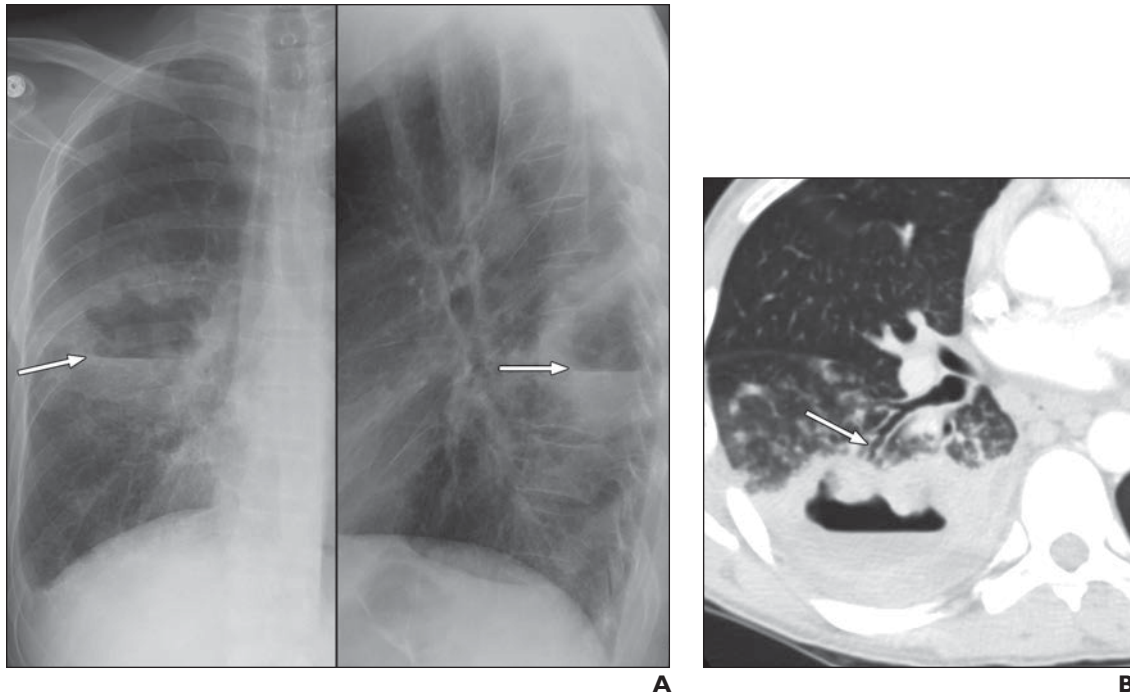


Fig. 8—35-year-old man with *Staphylococcus aureus* pneumonia forming lung abscess. Example of air-fluid level sign.

A, Posteroanterior (*left*) and lateral (*right*) radiographs show right lower lobe cavity with air-fluid level (*arrows*) of equal length on both orthogonal views. Thick, irregular wall typical of lung abscess is evident.

B, Axial CT image shows parenchymal location of right lower lobe cavity with air-fluid level, irregular internal contours, and associated bronchus (*arrow*) coursing to lesion.

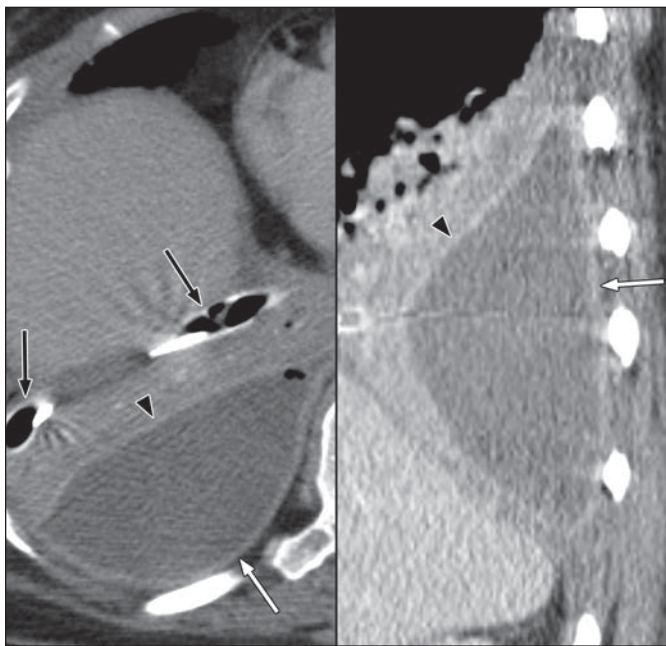


Fig. 9—48-year-old woman with empyema. Example of split-pleura sign. Axial (*left*) and sagittal (*right*) contrast-enhanced CT images show thickened visceral (*arrowhead*) and parietal (*white arrows*) pleura separated from their normal state of apposition (i.e., split) to surround loculated empyema. Adjacent atelectasis is evident in right lower lobe. Split-pleura sign is not specific for empyema but rather indicates presence of exudative effusion. Chest tube is incompletely visible (*black arrows*).

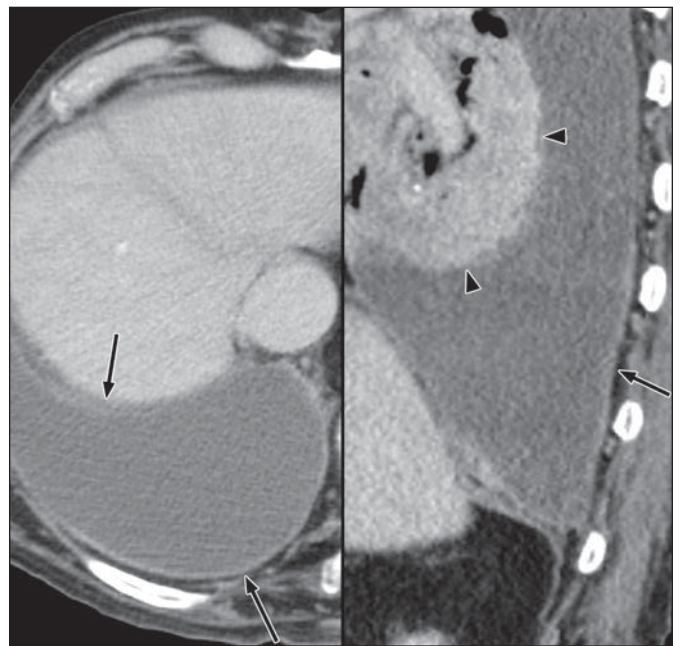


Fig. 10—65-year-old man with malignant pleural effusion. Example of split-pleura sign. Axial (*left*) and sagittal (*right*) contrast-enhanced CT images show thickening of visceral (*arrowheads*) and parietal (*arrows*) pleura with associated effusion. Split-pleura sign only indicates presence of exudative effusion and must be correlated with clinical findings and thoracentesis to establish accurate diagnosis.

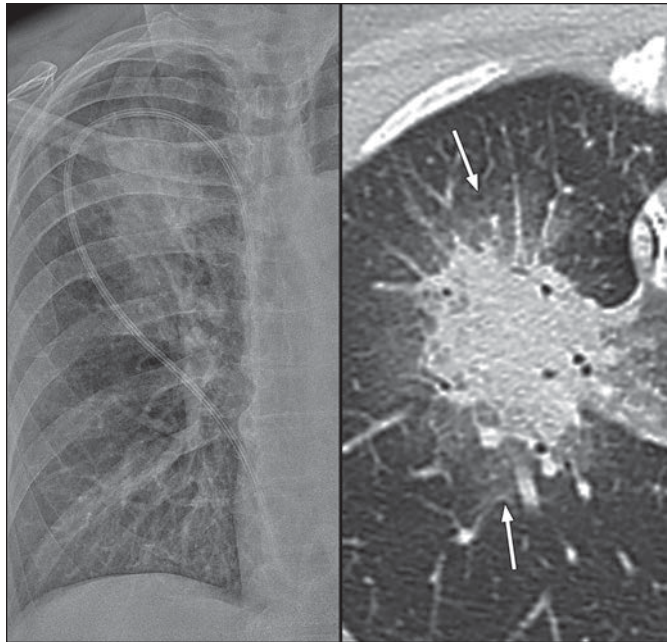


Fig. 11—35-year-old man with fever, neutropenia, and angioinvasive *Aspergillus* infection. Example of halo sign. Posteroanterior radiograph and axial CT image show right upper lobe mass with peripheral ground-glass opacity (arrows) constituting halo sign.



Fig. 12—47-year-old man with disseminated candidiasis. Example of halo sign. Axial CT image shows multiple bilateral pulmonary nodules with surrounding ground-glass opacity.

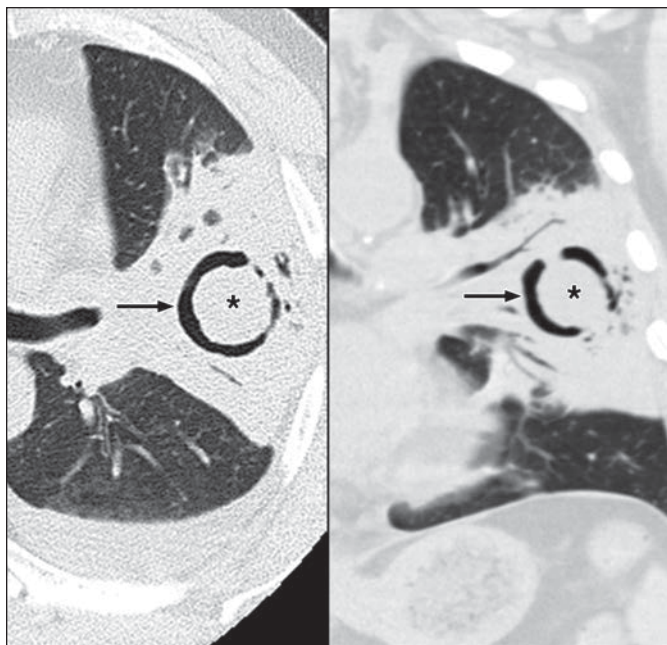


Fig. 13—38-year-old man with angioinvasive *Aspergillus* infection. Example of air crescent sign. Axial (left) and coronal (right) CT images show air crescent sign (arrows), which occurs in immunocompromised patients with recovering neutrophil levels. Intracavitary nodule (asterisks) represents necrotic lung tissue.

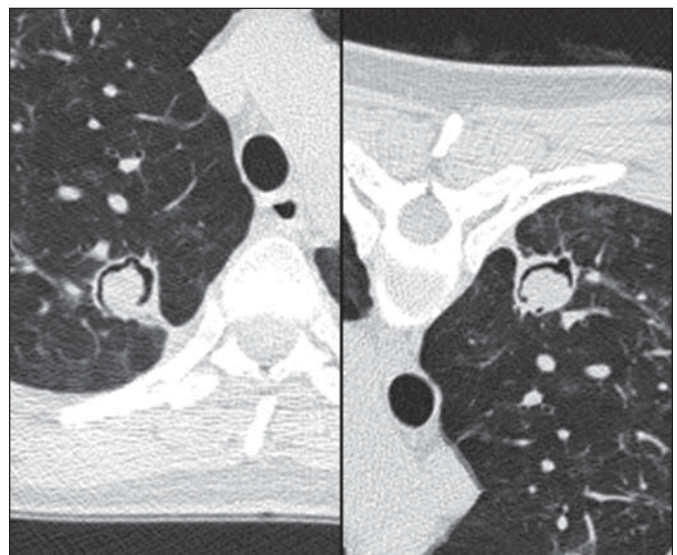
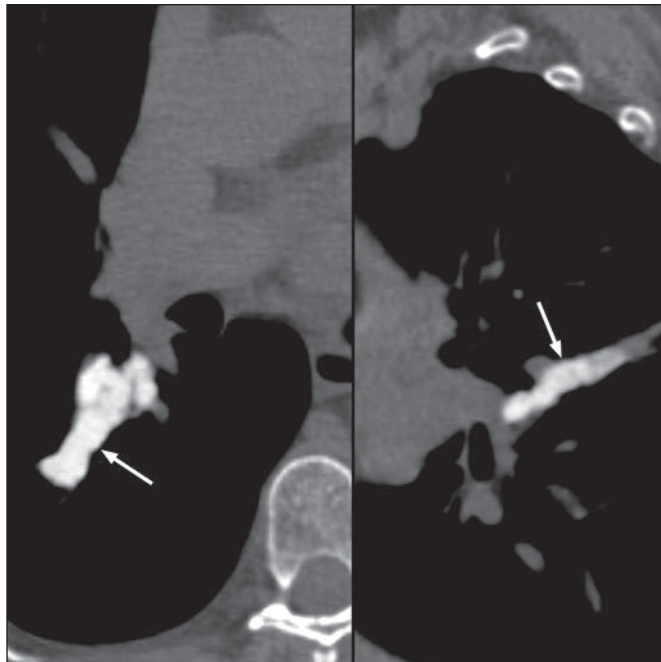
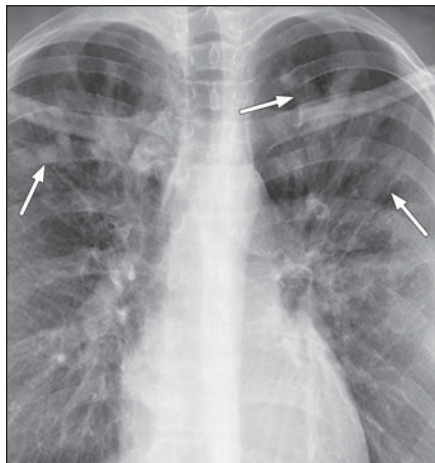


Fig. 14—65-year-old woman with intracavitary mycetoma. Example of air crescent or Monad sign. Axial supine (left) and prone (right) CT images show gravity dependence of fungal ball (mycetoma). Air crescent sign of mycetoma occurs in immunocompetent patients. Fungus ball develops within preexisting cavity, usually in association with tuberculosis or sarcoidosis.

Imaging Pulmonary Infection



A

B

Fig. 15—25-year-old woman with allergic bronchopulmonary aspergillosis (ABPA). Example of finger-in-glove sign. **A**, Posteroanterior radiograph shows branching tubular opacities (arrows) emanating from both hila. **B**, Unenhanced axial (left) and oblique sagittal (right) CT images show branching tubular opacities (arrows) with high attenuation. Opacities in ABPA are composed of hyphal masses, and mucoid impaction and may be calcified on CT images in as many as 28% of cases.

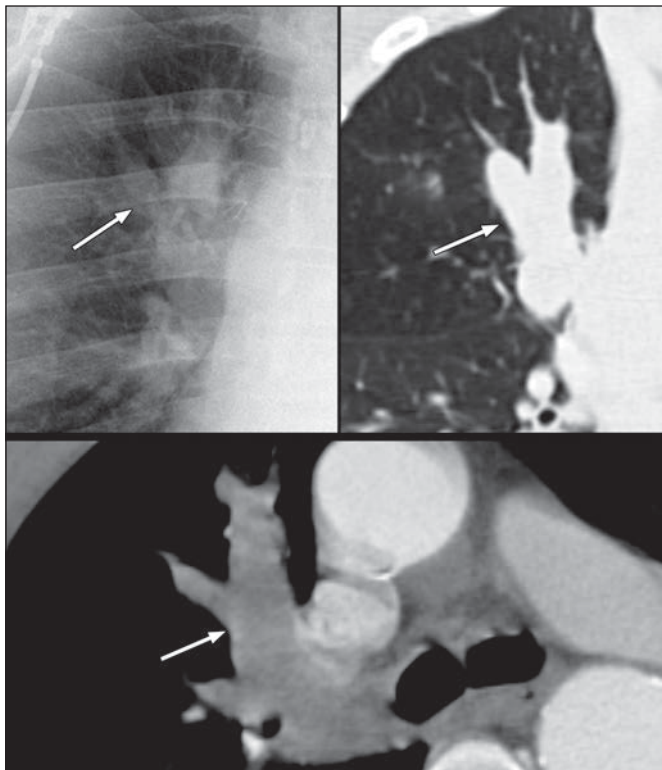


Fig. 16—63-year-old man with squamous cell lung cancer. Example of finger-in-glove sign. Posteroanterior radiograph (top left) and corresponding coronal (top right) and axial (bottom) CT images show branching tubular opacity (arrows) in right upper lobe. Proximal portion of branching opacity was FDG avid (not shown) and represented tumor, whereas rest of opacity represented mucoid impaction in dilated bronchus.

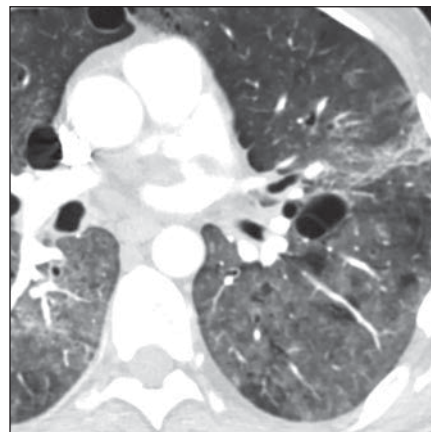


Fig. 17—24-year-old man with HIV infection and *Pneumocystis* pneumonia. Example of crazy-paving sign. Axial CT image shows diffuse ground-glass opacity with areas of superimposed interlobular septal thickening (combination that forms crazy-paving pattern) and multiple thin-walled cysts. In HIV-positive patient with dyspnea, findings are most consistent with *Pneumocystis* pneumonia.

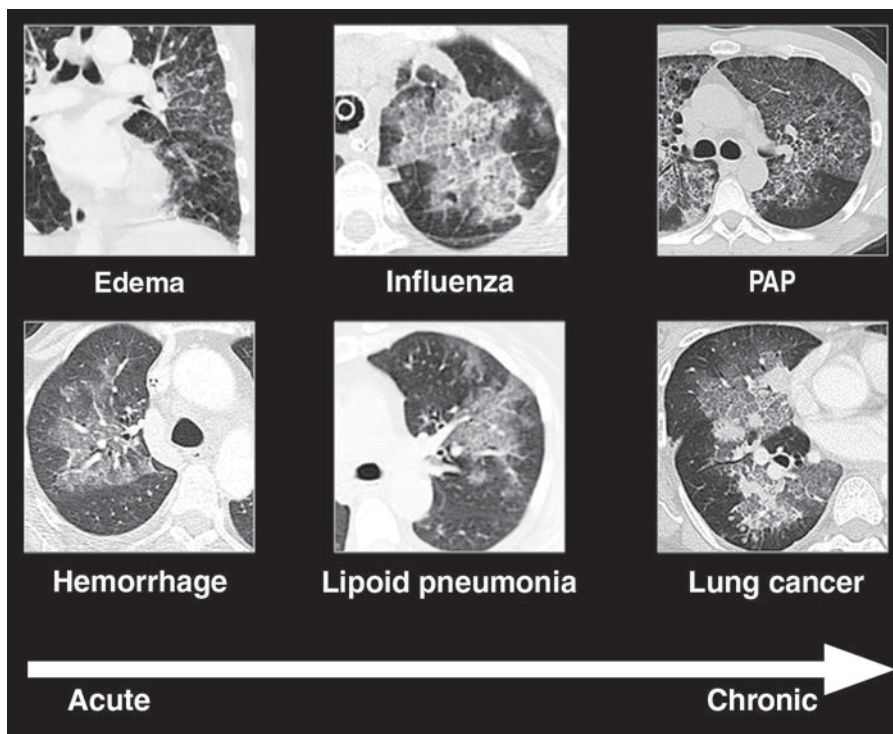


Fig. 18—CT scans show crazy-paving sign in patients with various disorders. Differential diagnostic considerations are influenced by patient's clinical presentation and disease course. In patients with acute symptoms, crazy-paving sign may represent pulmonary edema, pulmonary hemorrhage, or infection. In patients with chronic symptoms, crazy-paving sign may represent lipoid pneumonia, lung cancer, or pulmonary alveolar proteinosis (PAP).

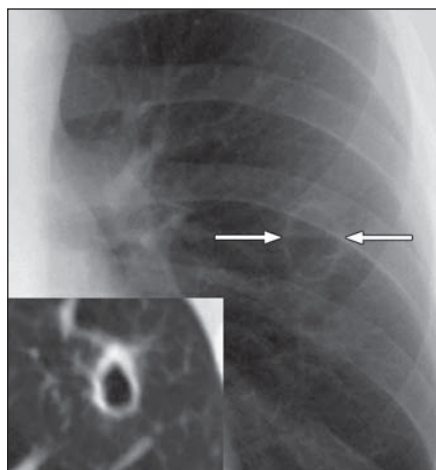


Fig. 19—55-year-old man with chronic coccidioidomycosis infection. Example of grape-skin sign. Posteroanterior radiograph shows thin-walled grape-skin cyst (arrows). Axial CT image (*inset*) shows that over time cavity may deflate and acquire slightly thicker wall.



Fig. 20—29-year-old man with AIDS (CD4 count, 10/ μ L) and disseminated histoplasmosis. Example of miliary pattern. Axial CT image shows multiple small pulmonary nodules distributed uniformly throughout both lungs. Some nodules are in contact with major fissure and subpleural lung and have no relation to secondary pulmonary lobules. Differential considerations for randomly distributed pulmonary nodules include miliary infection (e.g., tuberculosis, histoplasmosis), metastatic disease, and rarely sarcoidosis.

Imaging Pulmonary Infection

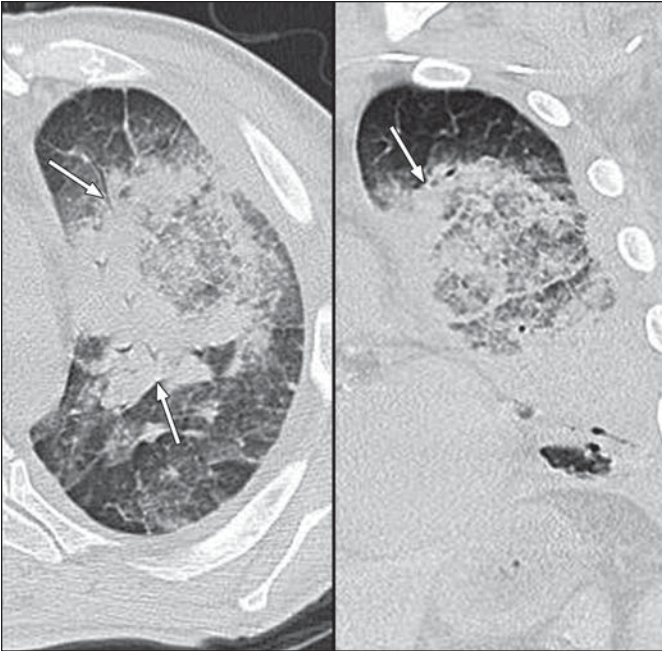


Fig. 21—44-year-old man with febrile neutropenia and pulmonary mucormycosis. Example of reverse halo and bird's nest signs. Axial (*left*) and coronal (*right*) CT images show peripheral rim of consolidation (*arrows*) surrounding central ground-glass opacity, reticulation, and nodularity. This appearance has been likened to bird's nest and reverse halo. Early diagnosis of mucormycosis pneumonia is imperative because standard voriconazole therapy is not effective for treatment. (Courtesy of Chou S, University of Washington, Seattle, WA)

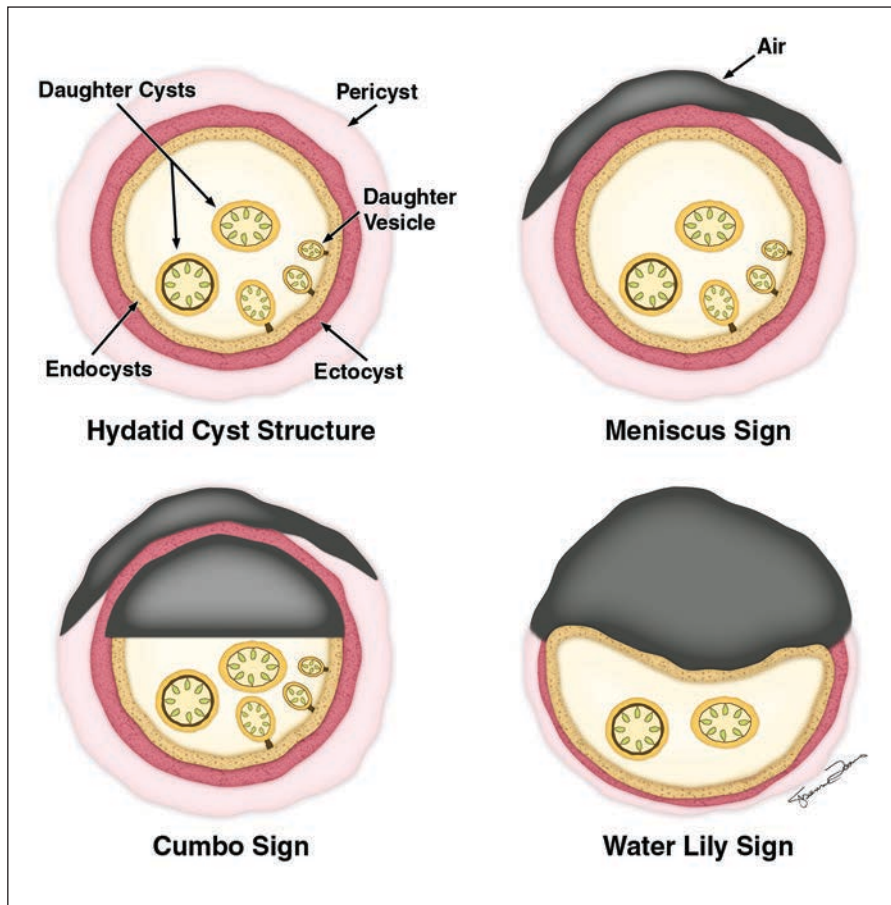


Fig. 22—Drawings show normal hydatid cyst and meniscus, Cumbo, and water lily signs. (Courtesy of Loomis S, REMS Media Services, Mass General Imaging, Boston, MA)

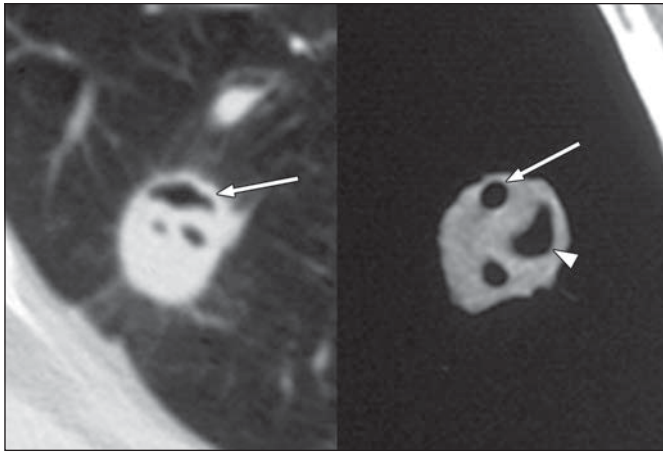


Fig. 23—49-year-old man with pulmonary hydatid disease. Example of meniscus (*left*) and Cumbo (*right*) signs. Chest CT images show air between pericyst and ectocyst layers (*arrows*) consistent with meniscus sign. Air-fluid level in endocyst (*arrowhead*) in combination with meniscus sign forms Cumbo sign. (Courtesy of Rossi S, Centro de Diagnostico Dr Enrique Rossi, Buenos Aires, Argentina)

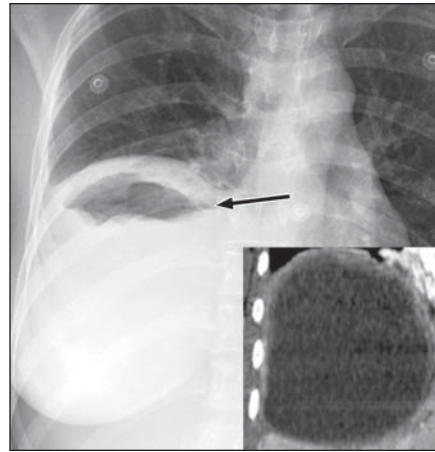


Fig. 24—27-year-old woman with pulmonary hydatid disease. Example of water lily sign. Posteroanterior radiograph shows large right lower lobe thick-walled cavity with lobulated air-soft-tissue interface representing floating endocyst (*arrow*). Coronal CT image (*inset*) from earlier examination shows unruptured cyst.

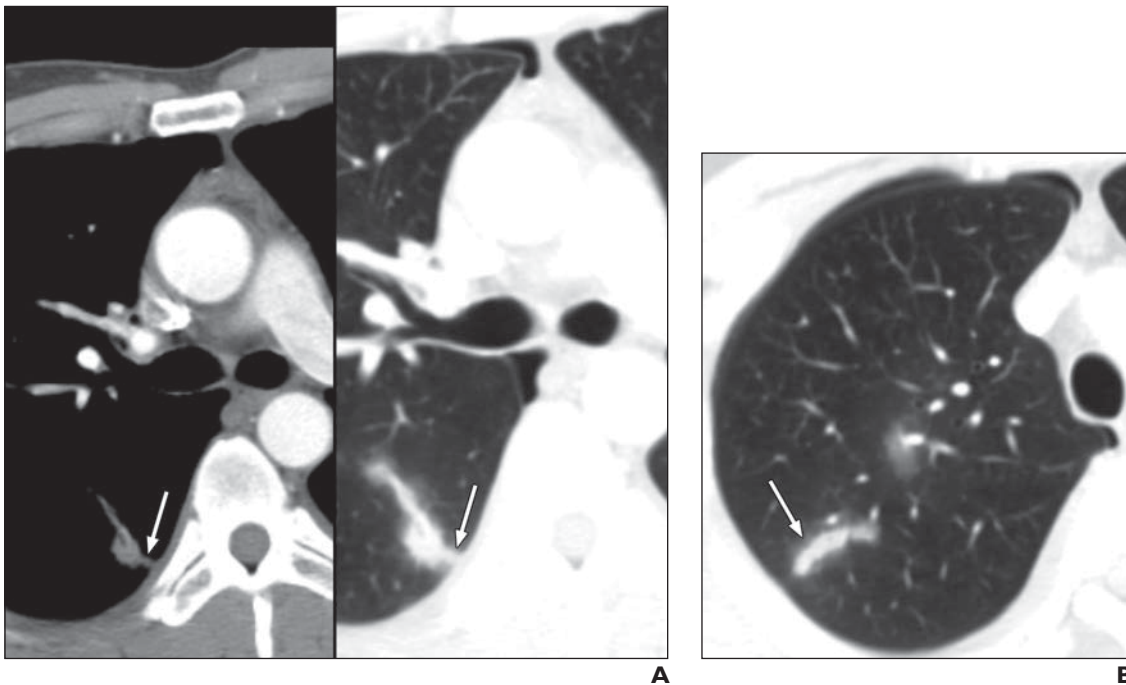


Fig. 25—32-year-old man with North American paragonimiasis after ingestion of raw crayfish. Example of burrow sign. (Courtesy of Henry T, Emory University, Atlanta, GA)

A, Axial CT images in soft-tissue (*left*) and lung (*right*) windows shows linear burrow track (*arrows*) extending from thickened pleura to pulmonary nodule.

B, Axial CT image shows long linear burrow track (*arrow*) in right upper lobe and small pneumothorax.

FOR YOUR INFORMATION

This article is available for CME and Self-Assessment (SA-CME) credit that satisfies Part II requirements for maintenance of certification (MOC). To access the examination for this article, follow the prompts associated with the online version of the article.